JOURNAL OF AGRICULTURAL AND FOOD CHEMISTRY

Article

pubs.acs.org/JAFC

Proteomic Study on Usnic-Acid-Induced Hepatotoxicity in Rats

Qian Liu,[†] Xiaoping Zhao,[‡,§] Xiaoyan Lu,[†] Xiaohui Fan,[†] and Yi Wang*[,†]

[†]Pharmaceutical Informatics Institute, College of Pharmaceutical Sciences, Zhejiang University, Hangzhou 310058, People's Republic of China

[‡]College of Preclinical Medicine, Zhejiang Chinese Medical University, Hangzhou 310053, People's Republic of China

[§]Tianjin State Key Laboratory of Modern Chinese Medicine, Tianjin University of Traditional Chinese Medicine, Tianjin 300193, People's Republic of China

ABSTRACT: Usnic acid, a lichen metabolite, is used as a dietary supplement for weight loss. However, clinical studies have shown that usnic acid causes hepatotoxicity. The present study aims to investigate the mechanism of usnic acid hepatotoxicity *in vivo*. Two-dimensional gel electrophoresis coupled with matrix-assisted laser desorption/ionization time-of-flight mass spectrometry was used to analyze the expression profiles of differentially regulated and expressed proteins in rat liver after usnic acid administration. The results reveal the differential expression of 10 proteins in usnic-acid-treated rats compared to the normal controls. These proteins are associated with oxidative stress, lipid metabolism, and several other molecular pathways. The endoplasmic reticulum and mitochondria may be the primary targets of usnic-acid-induced hepatotoxicity.

KEYWORDS: *Usnic acid, proteomics, hepatotoxicity*

INTRODUCTION

Obesity is increasingly becoming a global concern. Consequently, the number of natural products being used for their weight reduction effects is also increasing. Of these, fat burners are believed to raise metabolism, which, in turn, accelerates weight loss.[1] Usnic acid [2,6-diacetyl-7,9-dihydroxy-8,9b-dimethyl-1,3(2*H*,9b*H*)-dibenzo-furandione] is one of the most abundant and secondary metabolites of several lichen species.[2] It has two optical enantiomers, namely, (+) and (−), both of which exhibit similar physicochemical properties and unique biological properties.[3] Usnic acid has been traditionally used as an antimicrobial agent.[4,5] It is resistant to non-tuberculous mycobacteria and *Mycobacterium tuberculosis*,[6] dental plaque biofilm,[7] alga *Scenedesmus*,[8] and *Helicobacter pylori*.[9] The experimental antiproliferative and cytotoxic effects[5] of usnic acid significantly inhibited the proliferation and growth of two different human cancer cell lines.[10] Aside from the medical and cosmetic value of usnic acid in burn healing[11] and ultraviolet (UV)-radiation protection,[12] usnic acid is also widely used in fat-burning agents and as a food additive.[4] However, long-term treatment of usnic acid can result in serious side effects, particularly fulminant hepatic failure.[4,13] Unfortunately, the mechanisms of hepatotoxicity of usnic acid remain unknown.

Recent studies have shown that usnic acid reduces the viability of primary hepatocytes in rats.[14] Furthermore, hepatotoxicity was observed in mice orally treated with usnic acid.[15] In the present study, we investigated the possible mechanisms of usnic-acid-induced hepatotoxicity via two-dimensional gel electrophoresis (2DE) coupled with matrix-assisted laser desorption/ionization time-of-flight mass spectrometry (MALDI−TOF MS).

MATERIALS AND METHODS

Chemicals. (+)-Usnic acid was purchased from Lion Biological Technology Co., Ltd. (Zhengzhou, China, purity > 99%). The structure is shown in Figure 1.

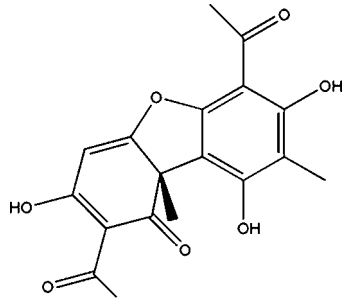

(+)-usnic acid

Figure 1. Chemical structural of (+)-usnic acid.

Materials. A protease inhibitor cocktail was purchased from Amresco (Solon, OH). The 2D cleanup kit was obtained from GE Healthcare (Amersham, Freiburg, Germany). Bovine serum albumin (BSA) was obtained from Sigma (St. Louis, MO). Sodium acetate, silver nitrate, and iodoacetamide were purchased from Hangzhou HaoTian Biotechnology Co., Ltd. (Hangzhou, China). Glycine, acrylamide, *N*,*N*′-methylenebisacrylamide, glycerol, tris-(hydroxymethyl)aminomethane (Tris), bromophenol blue, sodium dodecyl sulfate (SDS), ammonium persulfate (AP), *N*,*N*,*N*′,*N*′-tetramethylethyldiamide (TEMED), 1,4-dithiothreitol (DTT), 3-3-1-propane-sulfonate (CHAPS), carbamide (urea), ethylenediaminetetra-acetic acid (EDTA), sodium carbonate, agarose, and sodium

Received: November 16, 2011
Revised: July 4, 2012
Accepted: July 4, 2012
Published: July 4, 2012

thiosulfate were purchased from Shanghai Biotech Co., Ltd. (Shanghai, China). All other reagents were of analytical grade.

Animal Treatment Protocol. A total of 16 male Wistar rats (280−300 g, Silaike Co., Shanghai, China) were used. All rats were housed in cages in an environmentally controlled room. The rats were provided with standard chow and water *ad libitum*. The experimental procedures conform to the Guide for the Care and Use of Laboratory Animals (National Academy Press, Washington, D.C.) and the Animal Care and Use Committee of Zhejiang University. Usnic acid was dissolved in 1% carboxymethyl cellulose (CMC). The rats were divided equally into four groups, namely, normal control (NC), vehicle control (VC) (1% CMC, i.g.), low dose (LD) (100 mg kg^{-1} day^{-1} usnic acid, i.g.), and high dose (HD) (240 mg kg^{-1} day^{-1} usnic acid, i.g.). All animals were weighed and oral-gavaged once daily with a 1 mL/100 g dose of usnic acid. Liver samples were obtained and stored in 10% formaldehyde solution for histopathological examination or at −80 °C for proteomic analysis after 10 days of treatment. Notably, 2 rats in the HD group died just before sacrifice. We took their liver samples as well.

Histopathology. The liver samples were stained with hematoxylin and eosin (H&E). After fixation, the liver was embedded in paraffin and sectioned at 5 μm intervals. The tissue sections were repeatedly washed with decreasing concentrations of ethanol prior to feosin staining. The liver was then mounted, and its morphology was examined and imaged via microscopy (DMI6000 B microscope, Leica, Wetzlar, Germany).

Sample Preparation. The liver samples were smashed on ice and homogenized in a lysis buffer consisting of 8 mol/L urea, 2 mol/L thiourea, 4% CHAPS, 10 mmol/L Tris, and 5 μL/10 mL protease inhibitor cocktail. The resulting homogenates were centrifuged at 4 °C for 20 min. The supernate was removed, desalted with the 2D Cleanup Kit, and stored at −80 °C.

2DE. There were 4 groups and 4 animals in each group. The liver sample from each animal was performed by 2DE analysis. 2DE was performed as previously reported.[16,17] In the first-dimensional separation, 80 μg of protein was applied on an immobilized 24 cm nonlinear gradient strip (Amersham Biosciences) at pH 3−10. The strips were active during rehydration [rehydration solution: 2% CHAPS, 0.5% immobilized pH gradient (IPG) buffer, 0.02% bromophenol blue, 8 M urea, and 2.8 mg/mL DTT] for 12 h at 30 V in a hydration buffer. Focusing was performed under a pressure increase to 73 kV h.

The strips were then equilibrated in 30% (v/v) glycerol, 2% (w/v) SDS, 0.002% bromophenol blue, 50 mM Tris-HCl buffer (pH 8.8), 6 M urea, and 10 mg/mL DTT for 15 min. After the first equilibration, the strips were equilibrated in the second equilibration buffer for 15 min, in which DTT was replaced with 25 mg/mL iodoacetamide. In the second-dimensional separation, the strip was applied to a 12% SDS−polyacrylamide gel (200 × 260 × 1 mm^3) overlaid with agarose gel (0.5% agarose and 0.002% bromophenol blue in a standard SDS running buffer). The gels were run on an Ettan DALTsix electrophoresis system (Amersham Biosciences) at 5 W/gel for 1 h and then at 20 W/gel until bromophenol blue reached the bottom of the gel. The 2DE gels were silver-stained using previously described methods[17] but with modifications.

Quantitative Gel Pattern Analysis. The silver-stained gels were digitized using a Powerlook 2100XL (Umax, Hanchu, Taiwan) scanner. The gel images were analyzed using the Image Master 2D Platinum software (version 5, Amersham Biosciences, Piscataway, NJ). The intensity of the spot (%) represents the percentage of a protein in the total proteins. The cutoff for the differentially expressed proteins is 1.5-fold.

MALDI−TOF MS for Protein Identification. MALDI−TOF MS was performed as previously described.[17] In brief, the silver-stained proteins in the gels were cut out, destained, and digested with trypsin. The masses of the resulting peptides were determined using a 4700 Proteomics Analyzer (TOF/TOF) (Applied Biosystems, Foster City, CA). The peptide mass search was performed against an NCBInr2009 database using the GPS Explorer software (Applied Biosystems, Foster City, CA).

Western Blot Analysis of Differentially Expressed Proteins. Western blot was performed to confirm the quantitative changes in each identified protein. Three individual liver samples from each group were performed. The presence of heat-shock protein 60 (HSP60), apolipoprotein A-I (Apo A-I), mitogen-activated protein kinase activator with WD-repeat binding protein (MAWDBP), and transthyretin (TTR) was verified, and β-actin expression was used as an internal control. HSP60, Apo A-I, and MAWDBP were separated using 12% SDS−polyacrylamide gels and electrotransferred to nitrocellulose membranes (Bio-Rad Laboratories, Hercules, CA). TTR was separated by 15% SDS−polyacrylamide gel and transferred to a polyvinylidene fluoride (PVDF) membrane using the iBlot dry blotting system (Invitrogen, Carlsbad, CA). After the membranes were blocked for 2 h at room temperature, they were incubated overnight at 4 °C with primary antibodies: mouse anti-HSP60 (1:100; Sigma, St. Louis, MO), rabbit anti-Apo A-I (1:250; Bioss, Beijing, China), rabbit anti-MAWDBP (1:200; Bioss, Beijing, China), rabbit anti-TTR (1:200; Bioss, Beijing, China), and mouse anti-actin (1:1000; Santa Cruz, CA). The membranes were then washed and incubated with the corresponding horseradish peroxidase (HRP)-conjugated secondary antibodies at a 1:8000 dilution for 1.5 h at room temperature. Protein bands were visualized using the Immobilon Western Chemiluminescent HRP Substrate (Millipore Corporation) and captured on an X-ray film.

Data Analysis. All values are expressed as the mean ± standard deviation (SD). The difference in means between groups was determined using one-way analysis of variation (ANOVA). Values with $p < 0.05$ were considered statistically significant. All statistical analyses were performed using Minitab 14 (Mintab, Inc., State College, PA).

RESULTS AND DISCUSSION

Histopathology. HE staining was performed on the liver tissues for the histopathological observation. Normal liver morphology was observed in the VC group (Figure 2A). In the LD group (Figure 2B), a large number of hepatocytes were swollen and only a few displayed mild cytoplasmic vacuolation. In the HD group (Figure 2C), the hepatocytes exhibited widespread vacuolation degeneration and some hepatocytes showed hydropic degeneration.

2DE and MS Analysis. The liver proteins from rats treated with and without usnic acid were analyzed via 2DE. The protein abundance, which represents the relative intensity of the spots, was determined using the Image Master 2D Platinum. The means of the protein spots of the NC, VC, LD, and HD groups were 1189, 1060, 1187, and 1192, respectively. The differential protein spots are shown in Figure 3. Several protein spots that showed significant changes, such as those of HSP60, MAWDBP, endoplasmic reticulum protein 29 (ERp29), and peroxiredoxin 4 (Prx4), are shown in Figure 4.

A total of 10 protein spots dynamically changed after treatment with usnic acid. These markedly altered protein spots were excised from the 2DE gels and subjected to in-gel trypsin digestion for MALDI−TOF MS analysis. Among these differential proteins, six proteins were upregulated, including HSP60, glucose-regulated protein 75 (Grp75), MAWDBP, albumin, Apo A-I, and ferritin light chain. A total of four proteins were downregulated, namely, TTR, catechol-*O*-methyltransferase (COMT), ERp29, and Prx4 (Table 1).

Heat-shock proteins (HSPs) were detected in all organisms. These proteins were considered to be a family of highly conserved cellular chaperones that play key roles in the assembly, folding, and transport of proteins.[18] HSPs were induced under various abnormal conditions, such as oxidative stress,[19] which was regarded as the mechanism of toxicity of numerous chemicals.[20] HSP60 was known as a mitochondrial

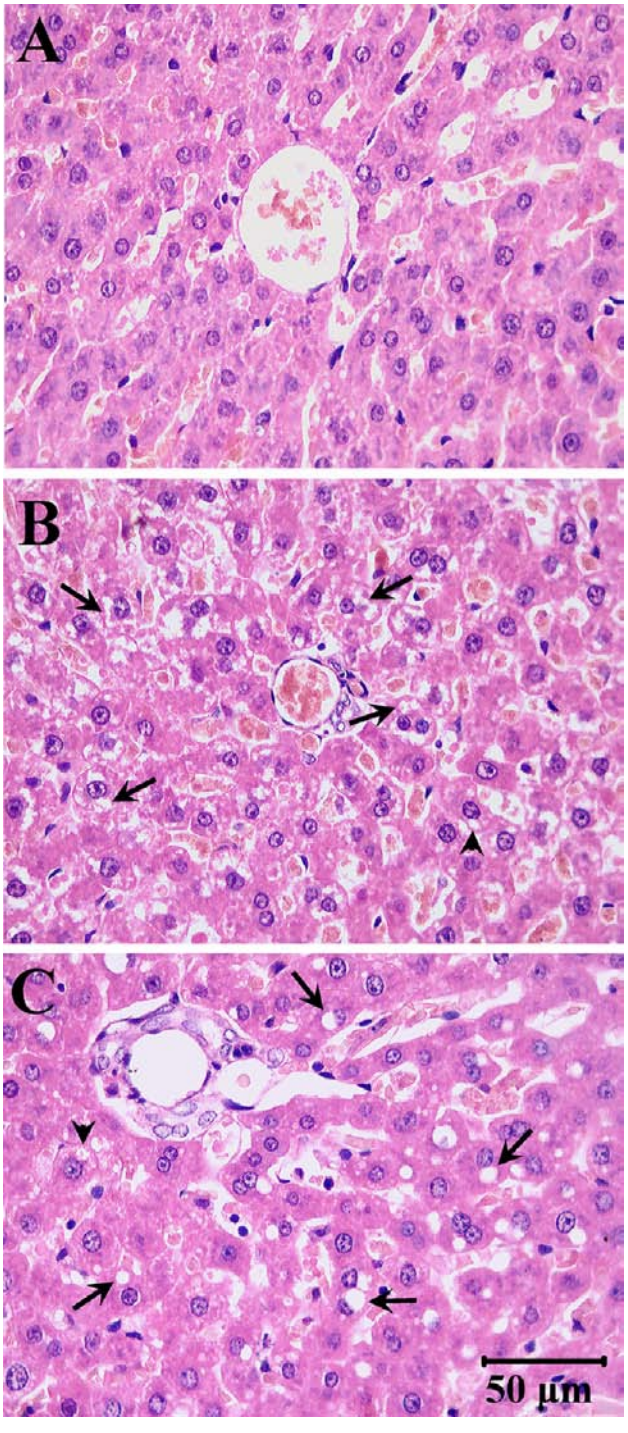

Figure 2. Histopathological examination. Micrographs of H&E staining for the (A) VC, (B) LD, and (C) HD groups. In the VC group, no obvious damages were detected. In the LD group, hepatocytes exhibited swollen (arrow) and mild cytoplasmic vacuolation (arrowhead). In the HD group, hepatocytes exhibited vacuolation degeneration (arrow) and hydropic degeneration (arrowhead). Magnification, 400×. The scale bar is 50 μm.

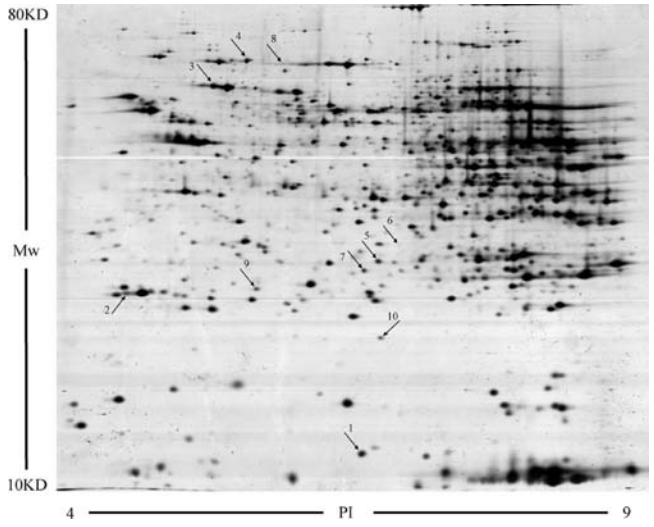

Figure 3. Representative 2D gel map of the rat liver sample. Proteins were stained by silver. Differential proteins were marked by an arrow and identified by MALDI−TOF MS. Numbered spots were identified and listed in Table 1.

protein[21] and plays an important role in the folding of key proteins, promotion of the proper assembly, and refolding of unfolded polypeptides generated under stress conditions in the mitochondria. In their proteomics study, Meneses-Lorente et al.[22] demonstrated that HSP60 was upregulated in rat liver after hepatocellular steatosis. Rezzani et al.[23] also showed that HSP60 levels increased in rat liver after cyclosporine A treatment. In the present study, HSP60 was also significantly upregulated in hepatocytes. The results indicated that the mechanism of hepatotoxicity of usnic acid may be through oxidative stress in the mitochondria.

MAWDBP was first identified as a binding partner of MAWD in 2001.[24] The downregulation of MAWDBP was reported in ethanol-fed[25] and diethyl-maleate-treated rat liver.[26] Its upregulation was also observed in streptozotocin-induced diabetic rat pancreas.[27] However, its detailed biological function and mechanisms remain unclear. In our findings, MAWDBP expression in rat liver significantly increased after usnic acid treatment. These results suggest that MAWDBP plays an important role in disrupting cellular homeostasis.

High-density lipoprotein (HDL) cholesterol levels were inversely related to the incidence rate of coronary heart disease. The increase in endogenous Apo A-I synthesis augmented the circulating HDL particles, which facilitated the movement of cholesterol mobilization.[28] Apo A-I removed excess cholesterol from tissues by acting as a co-factor for lecithin cholesterol acyltransferase.[29] Degoma et al. revealed that Apo A-I plays a key role in the treatment of atherothrombotic cardiovascular diseases.[30] Cho et al. showed that Apo A-I plays an important role in low *trans*-structured fats.[31] Usnic acid has been reported to upregulate several genes involved in fatty acid oxidation in mice.[32] In our findings, usnic acid treatment increased the Apo A-I levels in hepatocytes. This phenomenon may be correlated with the fat-burning effect of usnic acid.

The endoplasmic reticulum (ER) was a multifunctional organelle and played crucial roles in synthesizing secretory proteins and mobilizing calcium stores.[33] ERp29 was widely believed to be abundantly and ubiquitously expressed in the ER of animal cells. ERp29 was characterized in the tooth-enamel-producing cells and recognized as a general folding assistant for secretory proteins.[34] Shnyder et al. suggested that ERp29 was primarily involved in the early phases of secretory protein processing.[34] In the current study, ERp29 was significantly decreased in the usnic-acid-treated HD group compared to the NC group. The downregulation of ERp29 occurred because of

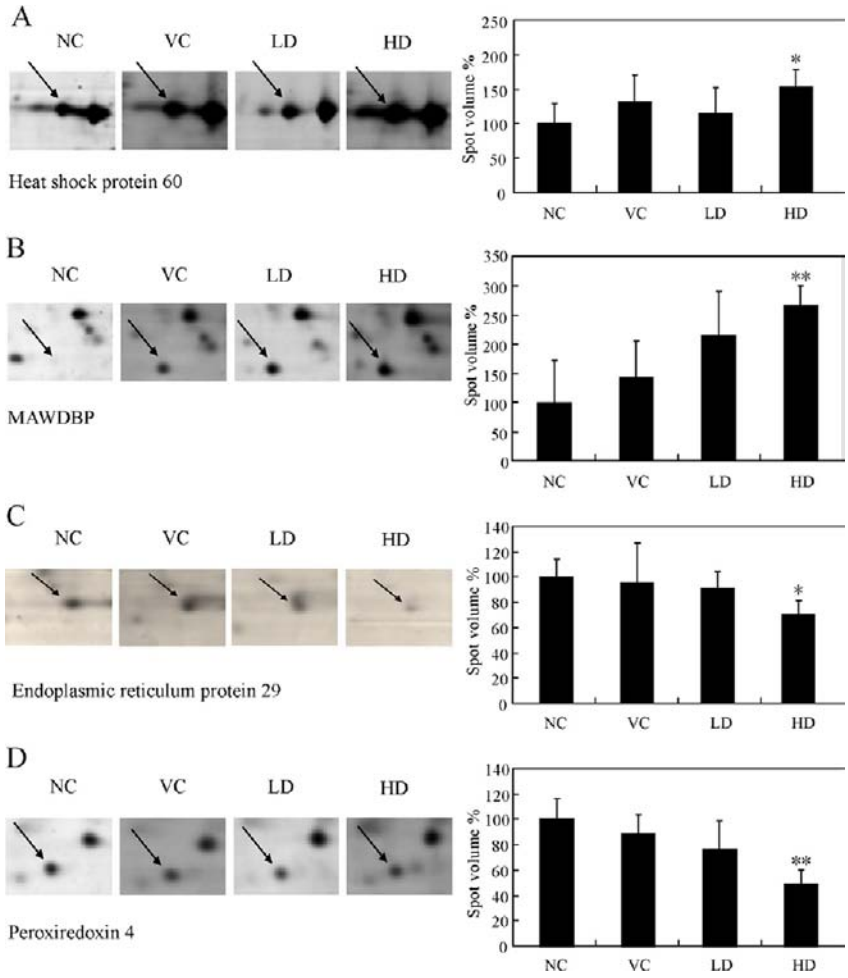

Figure 4. Some examples of differential proteins in NC, VC, LD, and HD groups. Data are expressed as the mean ± SD (n = 4 for each experimental group). (*) $p < 0.05$ versus NC. (**) $p < 0.01$ versus NC.

Table 1. Characterization of the Identified Altered Proteins of Rat Liver

							relative spot intensity percentage (NC, 100)		
spot number[a]	protein identity	NCBI accession number	experimental values (theoretical values) pI/kDa	peptide count	percentage of coverage (%)	score	VC	LD	HD
1	TTR	136467	5.77/16 (5.08/16)	8	96.6	208	113 ± 66.5	86 ± 36.6	52 ± 29.3
2	COMT	209156404	5.11/25 (5.01/29)	5	34.5	69	82 ± 33.1	85 ± 32.1	39 ± 10.2
3	HSP60	56383	5.91/61 (5.69/62)	18	45.2	333	130 ± 39.3	114 ± 37.2	152 ± 26.4[b]
4	Grp75	1000439	5.87/74 (5.57/69)	22	43.6	462	100 ± 26.7	74 ± 41.0	117 ± 39.2
5	ERp29	16758848	6.23/29 (6.78/29)	6	27.3	137	95 ± 31.8	91 ± 13.7	71 ± 10.8*
6	MAWDBP	19743770	6.54/32 (6.53/32)	8	38.5	79	145 ± 63.0	217 ± 78.4	269 ± 36.7[c]
7	Prx4	16758274	6.18/31 (6.67/31)	6	27.1	124	88 ± 14.8	76 ± 22.4	48 ± 11.8[c]
8	albumin	149033753	6.09/69 (5.92/69)	10	22.0	106	98 ± 28.8	102 ± 42.4	147 ± 74.9
9	Apo A-I	2145143	5.51/30 (5.38/30)	11	44.6	68	63 ± 8.4	97 ± 52.5	122 ± 27.1
10	ferritin light chain	204123	5.99/21 (5.72/28)	7	51.9	304	69 ± 9.7	72 ± 15.3	128 ± 28.6

[a]The marked spot number. [b]$p < 0.05$ compared to the NC group. [c]$p < 0.01$ compared to the NC group.

ER stress.[35] ER and ERp29 are therefore potentially involved in the metabolic processes of usnic acid.

Peroxiredoxins (Prxs) were a family of multifunctional redox proteins with thioredoxin-dependent peroxidases that catalyze the reduction of peroxides and peroxynitrite.[36] Prx4 acts as a regulatory factor for nuclear factor κB (NF-κB) within the cells.[37] It is an ER-resident protein[38] and present in most tissues as a secretory protein.[39] Iuchi et al. showed that spermatogenic cells are more prone to death under oxidative damage without Prx4 compared to their wild-type counterparts.[40] Our results indicate that the Prx4 levels in rat hepatocytes dramatically declined after usnic acid administration, suggesting that Prx4 secretion may be perturbed by usnic acid.

Western Blot Validation. Western blot was used to verify the differentially expressed proteins that were identified via MS.

dx.doi.org/10.1021/jf2046834 | J. Agric. Food Chem. 2012, 60, 7312–7317

HSP60, Apo A-I, MAWDBP, and TTR were selected and subjected to western blot analysis. Figure 5 shows the western

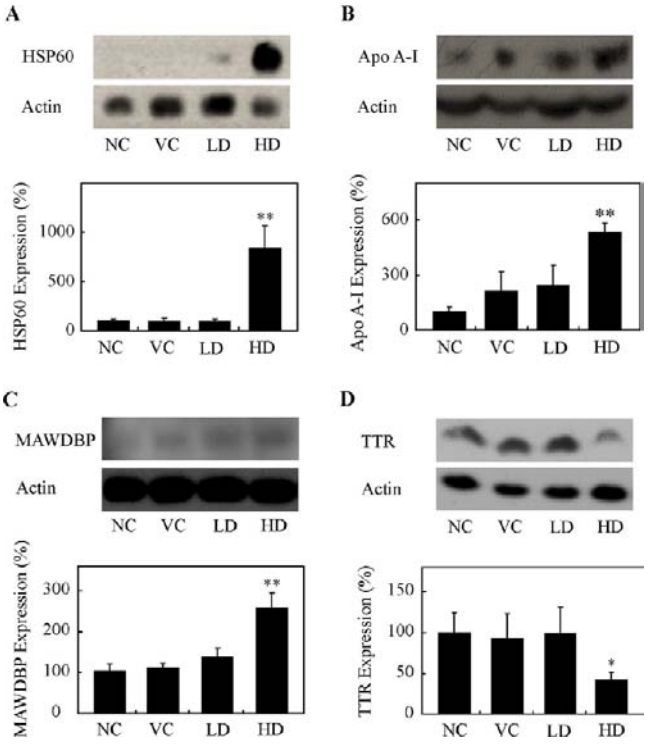

Figure 5. Western blot analysis results confirm the significant changes in the HSP60 and Apo A-I levels in the NC, VC, LD, and HD groups, as observed via 2DE. (A) Western blot bands of HSP60 and β-actin in the liver, as well as the semi-quantitative data for the HSP60 protein. (B) Western blot bands of Apo A-I and β-actin in the liver, as well as the semi-quantitative data for the Apo A-I protein. (C) Western blot bands of MAWDBP and β-actin in the liver, as well as the semi-quantitative data for the MAWDBP protein. (D) Western blot bands of TTR and β-actin in the liver, as well as the semi-quantitative data for the TTR protein. (*) $p < 0.05$ versus NC. (**) $p < 0.01$ versus NC.

blot bands of HSP60, Apo A-I, MAWDBP, TTR, and β-actin in the liver. The HSP60, Apo A-I, and MAWDBP levels in the usnic-acid-treated HD group increased compared to those in the NC group. The TTR level decreased in the HD group compared to the NC group. These results were consistent with the 2DE data.

An *in vitro* study showed that usnic acid induces cytotoxicity,[14] oxidative stress,[41] uncoupling of oxidative phosphorylation,[5] and cell membrane damage in hepatocytes.[42] Our *in vivo* study shows that cytotoxicity and oxidative stress were involved in usnic-acid-induced hepatotoxicity. Moreover, previous studies from our laboratory had shown that usnic acid administration led to toxicity in rat liver.[43] Lu et al. showed that usnic acid can induce mitochondrial uncoupling, inhibit mitochondrial function, induce oxidative stress, and eventually lead to cell death.[43] In the present study, usnic acid modulated a mass of proteins involved in oxidative stress, lipid metabolism, apoptosis, and some currently unknown processes. Our study suggested that the ER and mitochondria were the primary targets of usnic acid. The downregulation of Prx4 may be related to apoptosis because of its regulatory effect on NF-κB. Furthermore, the lipid metabolism function of usnic acid may be a result of the upregulation of Apo A-I. Although the usnic-acid-treated rat livers did not exhibit significant changes according to the proteomics approach, the results obtained from this study are nonetheless valuable. The interaction between the aforementioned proteins and the precise mechanism of usnic acid *in vivo* require further investigation. In addition, genomic, transcriptomic, and metabonomic data should be integrated using computational approaches.

AUTHOR INFORMATION

Corresponding Author

*Telephone/Fax: 86-571-88208426. E-mail: mysky@zju.edu.cn.

Funding

This work was supported by the National Key Scientific and Technological Project of China (2012ZX09505001-001), the National Natural Science Foundation of China (81173465), and the Fundamental Research Funds for the Central Universities.

Notes

The authors declare no competing financial interest.

ABBREVIATIONS USED

2DE, two-dimensional gel electrophoresis; MALDI−TOF MS, matrix-assisted laser desorption/ionization time-of-flight mass spectrometry; BSA, bovine serum albumin; Tris, Tris(hydroxymethyl)aminomethane; SDS, sodium dodecyl sulfonate; AP, ammonium persulfate; TEMED, *N,N,N′,N′*-tetramethylethyldiamide; DTT, 1,4-dithiothreitol; CHAPS, 3-3-1-propane-sulfonate; urea, carbamide; EDTA, ethylenediaminetetraacetic acid; NC, normal control; VC, vehicle control; LD, low dose; HD, high dose; H&E, hematoxylin and eosin; HSP60, heat-shock protein 60; Grp75, glucose-regulated protein 75; MAWDBP, mitogen-activated protein kinase activator with WD-repeat binding protein; Apo A-I, apolipoprotein A-I; TTR, transthyretin; COMT, catechol-*O*-methyltransferase; ERp29, endoplasmic reticulum protein 29; Prx4, peroxiredoxin 4; HSP, heat-shock protein; HDL, high-density lipoprotein; ER, endoplasmic reticulum; Prx, peroxiredoxin

REFERENCES

(1) Yellapu, R. K.; Mittal, V.; Grewal, P.; Fiel, M.; Schiano, T. Acute liver failure caused by 'fat burners' and dietary supplements: A case report and literature review. *Can. J. Gastroenterol.* **2011**, *25*, 157−160.

(2) Ingolfsdottir, K. Usnic acid. *Phytochemistry* **2002**, *61*, 729−736.

(3) Roach, J. A.; Musser, S. M.; Morehouse, K.; Woo, J. Y. Determination of usnic acid in lichen toxic to elk by liquid chromatography with ultraviolet and tandem mass spectrometry detection. *J. Agric. Food Chem.* **2006**, *54*, 2484−2490.

(4) Guo, L.; Shi, Q.; Fang, J. L.; Mei, N.; Ali, A. A.; Lewis, S. M.; Leakey, J. E.; Frankos, V. H. Review of usnic acid and *Usnea barbata* toxicity. *J. Environ. Sci. Health, Part C: Environ. Carcinog. Ecotoxicol. Rev.* **2008**, *26*, 317−338.

(5) Ivanova, V.; Backor, M.; Dahse, H. M.; Graefe, U. Molecular structural studies of lichen substances with antimicrobial, antiproliferative, and cytotoxic effects from *Parmelia subrudecta*. *Prep. Biochem. Biotechnol.* **2010**, *40*, 377−388.

(6) Ramos, D. F.; Almeida da Silva, P. E. Antimycobacterial activity of usnic acid against resistant and susceptible strains of *Mycobacterium tuberculosis* and non-tuberculous mycobacteria. *Pharm. Biol.* **2010**, *48*, 260−263.

(7) Chifiriuc, M. C.; Ditu, L. M.; Oprea, E.; Litescu, S.; Bucur, M.; Marutescu, L.; Enache, G.; Saviuc, C.; Burlibasa, M.; Traistaru, T.; Tanase, G.; Lazar, V. In vitro study of the inhibitory activity of usnic acid on dental plaque biofilm. *Rom. Arch. Microbiol. Immunol.* **2009**, *68*, 215−222.

(8) Backor, M.; Klemova, K.; Backorova, M.; Ivanova, V. Comparison of the phytotoxic effects of usnic acid on cultures of free-living alga *Scenedesmus quadricauda* and aposymbiotically grown lichen photobiont *Trebouxia erici*. *J. Chem. Ecol.* **2010**, *36*, 405−411.
(9) Safak, B.; Ciftci, I. H.; Ozdemir, M.; Kiyildi, N.; Cetinkaya, Z.; Aktepe, O. C.; Altindis, M.; Asik, G. In vitro anti-*Helicobacter pylori* activity of usnic acid. *Phytother. Res.* **2009**, *23*, 955−957.
(10) Einarsdottir, E.; Groeneweg, J.; Bjornsdottir, G. G.; Harethardottir, G.; Omarsdottir, S.; Ingolfsdottir, K.; Ogmundsdottir, H. M. Cellular mechanisms of the anticancer effects of the lichen compound usnic acid. *Planta Med.* **2010**, *76*, 969−974.
(11) Nunes, P. S.; Albuquerque, R. L., Jr.; Cavalcante, D. R.; Dantas, M. D.; Cardoso, J. C.; Bezerra, M. S.; Souza, J. C.; Serafini, M. R.; Quitans, L. J., Jr.; Bonjardim, L. R.; Araujo, A. A. Collagen-based films containing liposome-loaded usnic acid as dressing for dermal burn healing. *J. Biomed. Biotechnol.* **2011**, *2011*, 761593.
(12) Kohlhardt-Floehr, C.; Boehm, F.; Troppens, S.; Lademann, J.; Truscott, T. G. Prooxidant and antioxidant behaviour of usnic acid from lichens under UVB-light irradiation—Studies on human cells. *J. Photochem. Photobiol., B* **2010**, *101*, 97−102.
(13) Stickel, F.; Kessebohm, K.; Weimann, R.; Seitz, H. K. Review of liver injury associated with dietary supplements. *Liver Int.* **2011**, *31*, 595−605.
(14) Sonko, B. J.; Schmitt, T. C.; Guo, L.; Shi, Q.; Boros, L. G.; Leakey, J. E.; Beger, R. D. Assessment of usnic acid toxicity in rat primary hepatocytes using ^{13}C isotopomer distribution analysis of lactate, glutamate and glucose. *Food Chem. Toxicol.* **2011**, *49*, 2968−2974.
(15) Cheng, Y. B.; Wei, L. L.; Gu, N.; Si, K. W.; Shi, L.; Li, X. Q.; Li, C.; Yuan, Y. K. Oral acute toxicity of (+)-usnic acid in mice and its cytotoxicity in rat cardiac fibroblasts. *Nanfang Yike Daxue Xuebao* **2009**, *29*, 1749−1751.
(16) Fountoulakis, M.; Suter, L. Proteomic analysis of the rat liver. *J. Chromatogr., B: Anal. Technol. Biomed. Life Sci.* **2002**, *782*, 197−218.
(17) Wang, Y.; Liu, L.; Hu, C.; Cheng, Y. Effects of Salviae Mitiorrhizae and Cortex Moutan extract on the rat heart after myocardial infarction: A proteomic study. *Biochem. Pharmacol.* **2007**, *74*, 415−424.
(18) Feder, M. E.; Hofmann, G. E. Heat-shock proteins, molecular chaperones, and the stress response: Evolutionary and ecological physiology. *Annu. Rev. Physiol.* **1999**, *61*, 243−282.
(19) Chairi, H.; Fernandez-Diaz, C.; Navas, J. I.; Manchado, M.; Rebordinos, L.; Blasco, J. In vivo genotoxicity and stress defences in three flatfish species exposed to $CuSO_4$. *Ecotoxicol. Environ. Saf.* **2010**, *73*, 1279−1285.
(20) Stacey, N. H.; Klaassen, C. D. Inhibition of lipid peroxidation without prevention of cellular injury in isolated rat hepatocytes. *Toxicol. Appl. Pharmacol.* **1981**, *58*, 8−18.
(21) Arya, R.; Mallik, M.; Lakhotia, S. C. Heat shock genes—Integrating cell survival and death. *J. Biosci.* **2007**, *32*, 595−610.
(22) Meneses-Lorente, G.; Guest, P. C.; Lawrence, J.; Muniappa, N.; Knowles, M. R.; Skynner, H. A.; Salim, K.; Cristea, I.; Mortishire-Smith, R.; Gaskell, S. J.; Watt, A. A proteomic investigation of drug-induced steatosis in rat liver. *Chem. Res. Toxicol.* **2004**, *17*, 605−612.
(23) Rezzani, R.; Buffoli, B.; Rodella, L.; Stacchiotti, A.; Bianchi, R. Protective role of melatonin in cyclosporine A-induced oxidative stress in rat liver. *Int. Immunopharmacol.* **2005**, *5*, 1397−1405.
(24) Iriyama, C.; Matsuda, S.; Katsumata, R.; Hamaguchi, M. Cloning and sequencing of a novel human gene which encodes a putative hydroxylase. *J. Hum. Genet.* **2001**, *46*, 289−292.
(25) Shi, L.; Wang, Y.; Tu, S.; Li, X.; Sun, M.; Srivastava, S.; Xu, N.; Bhatnagar, A.; Liu, S. The responses of mitochondrial proteome in rat liver to the consumption of moderate ethanol: The possible roles of aldo−keto reductases. *J. Proteome Res.* **2008**, *7*, 3137−3145.
(26) Yamauchi, S.; Kiyosawa, N.; Ando, Y.; Watanabe, K.; Niino, N.; Ito, K.; Yamoto, T.; Manabe, S.; Sanbuissho, A. Hepatic transcriptome and proteome responses against diethyl maleate-induced glutathione depletion in the rat. *Arch. Toxicol.* **2011**, *85*, 1045−1056.
(27) Kim, S. W.; Hwang, H. J.; Baek, Y. M.; Lee, S. H.; Hwang, H. S.; Yun, J. W. Proteomic and transcriptomic analysis for streptozotocin-induced diabetic rat pancreas in response to fungal polysaccharide treatments. *Proteomics* **2008**, *8*, 2344−2361.
(28) Nicholls, S. J.; Gordon, A.; Johansson, J.; Wolski, K.; Ballantyne, C. M.; Kastelein, J. J.; Taylor, A.; Borgman, M.; Nissen, S. E. Efficacy and safety of a novel oral inducer of apolipoprotein a-I synthesis in statin-treated patients with stable coronary artery disease a randomized controlled trial. *J. Am. Coll. Cardiol.* **2011**, *57*, 1111−1119.
(29) Phillips, M. C.; Gillotte, K. L.; Haynes, M. P.; Johnson, W. J.; Lund-Katz, S.; Rothblat, G. H. Mechanisms of high density lipoprotein-mediated efflux of cholesterol from cell plasma membranes. *Atherosclerosis* **1998**, *137* (Supplement), S13−S17.
(30) Degoma, E. M.; Rader, D. J. Novel HDL-directed pharmacotherapeutic strategies. *Nat. Rev. Cardiol.* **2011**, *8*, 266−277.
(31) Cho, Y. Y.; Kwon, E. Y.; Kim, H. J.; Jeon, S. M.; Lee, K. T.; Choi, M. S. Differential effect of corn oil-based low *trans* structured fat on the plasma and hepatic lipid profile in an atherogenic mouse model: Comparison to hydrogenated trans fat. *Lipids Health Dis.* **2011**, *10*, 15.
(32) Joseph, A.; Lee, T.; Moland, C. L.; Branham, W. S.; Fuscoe, J. C.; Leakey, J. E.; Allaben, W. T.; Lewis, S. M.; Ali, A. A.; Desai, V. G. Effect of (+)-usnic acid on mitochondrial functions as measured by mitochondria-specific oligonucleotide microarray in liver of B6C3F1 mice. *Mitochondrion* **2009**, *9*, 149−158.
(33) Hubbard, M. J.; Mangum, J. E.; McHugh, N. J. Purification and biochemical characterization of native ERp29 from rat liver. *Biochem. J.* **2004**, *383*, 589−597.
(34) Shnyder, S. D.; Hubbard, M. J. ERp29 is a ubiquitous resident of the endoplasmic reticulum with a distinct role in secretory protein production. *J. Histochem. Cytochem.* **2002**, *50*, 557−566.
(35) Sanchez-Quiles, V.; Santamaria, E.; Segura, V.; Sesma, L.; Prieto, J.; Corrales, F. J. Prohibitin deficiency blocks proliferation and induces apoptosis in human hepatoma cells: Molecular mechanisms and functional implications. *Proteomics* **2010**, *10*, 1609−1620.
(36) Rhee, S. G.; Chae, H. Z.; Kim, K. Peroxiredoxins: A historical overview and speculative preview of novel mechanisms and emerging concepts in cell signaling. *Free Radical Biol. Med.* **2005**, *38*, 1543−1552.
(37) Jin, D. Y.; Chae, H. Z.; Rhee, S. G.; Jeang, K. T. Regulatory role for a novel human thioredoxin peroxidase in NF-κB activation. *J. Biol. Chem.* **1997**, *272*, 30952−30961.
(38) Immenschuh, S.; Baumgart-Vogt, E. Peroxiredoxins, oxidative stress, and cell proliferation. *Antioxid. Redox Signaling* **2005**, *7*, 768−777.
(39) Fujii, J.; Ikeda, Y. Advances in our understanding of peroxiredoxin, a multifunctional, mammalian redox protein. *Redox Rep.* **2002**, *7*, 123−130.
(40) Iuchi, Y.; Okada, F.; Tsunoda, S.; Kibe, N.; Shirasawa, N.; Ikawa, M.; Okabe, M.; Ikeda, Y.; Fujii, J. Peroxiredoxin 4 knockout results in elevated spermatogenic cell death via oxidative stress. *Biochem. J.* **2009**, *419*, 149−158.
(41) Han, D.; Matsumaru, K.; Rettori, D.; Kaplowitz, N. Usnic acid-induced necrosis of cultured mouse hepatocytes: Inhibition of mitochondrial function and oxidative stress. *Biochem. Pharmacol.* **2004**, *67*, 439−451.
(42) Pramyothin, P.; Janthasoot, W.; Pongnimitprasert, N.; Phrukudom, S.; Ruangrungsi, N. Hepatotoxic effect of (+)usnic acid from *Usnea siamensis* Wainio in rats, isolated rat hepatocytes and isolated rat liver mitochondria. *J. Ethnopharmacol.* **2004**, *90*, 381−387.
(43) Lu, X.; Zhao, Q.; Tian, Y.; Xiao, S.; Jin, T.; Fan, X. A metabonomic characterization of (+)-usnic acid-induced liver injury by gas chromatography−mass spectrometry-based metabolic profiling of the plasma and liver in rat. *Int. J. Toxicol.* **2011**, *30*, 478−491.